



**Associated conference:** 5th International Small Sample Test Techniques Conference

**Conference location:** Swansea University, Bay Campus

**Conference date:** 10th - 12 July 2018

---

**How to cite:** Prakash, R.V., Madhavan, K., Prakash, A.R., Sandhya, R. & Reddy, G.V.P. 2018. Fatigue response evaluation of stainless steel SS 304 L(N) and SS 316 L(N) through cyclic ball indentation studies. *Ubiquity Proceedings*, 1(S1): 38 DOI: <https://doi.org/10.5334/uproc.38>

**Published on:** 10 September 2018

---

**Copyright:** © 2018 The Author(s). This is an open-access article distributed under the terms of the Creative Commons Attribution 4.0 International License (CC-BY 4.0), which permits unrestricted use, distribution, and reproduction in any medium, provided the original author and source are credited. See <http://creativecommons.org/licenses/by/4.0/>.

**UBIQUITY PROCEEDINGS**



<https://ubiquityproceedings.com>

# Fatigue response evaluation of stainless steel SS 304 L(N) and SS 316 L(N) through cyclic ball indentation studies

R.V. Prakash<sup>1\*</sup>, K. Madhavan<sup>2</sup>, A.R. Prakash<sup>3</sup>, R. Sandhya<sup>4</sup> and G.V.P. Reddy<sup>4</sup>

<sup>1</sup> Indian Institute of Technology Madras, Chennai 600036, India; [raghuprakash@iitm.ac.in](mailto:raghuprakash@iitm.ac.in)

<sup>2</sup> SASTRA University, Thanjavur 613401, India; [krishnamadhavan007@gmail.com](mailto:krishnamadhavan007@gmail.com)

<sup>3</sup> National Institute of Technology, Tiruchirappalli 620015, India; [anirudh.kv.iit@gmail.com](mailto:anirudh.kv.iit@gmail.com)

<sup>4</sup> Indira Gandhi Centre for Atomic Research, Kalpakkam 603102, India; [san@igcar.gov.in](mailto:san@igcar.gov.in); [prasadreddy@igcar.gov.in](mailto:prasadreddy@igcar.gov.in)

\* Correspondence: [raghuprakash@iitm.ac.in](mailto:raghuprakash@iitm.ac.in); [raghu.v.prakash@gmail.com](mailto:raghu.v.prakash@gmail.com); Tel.: +91-442-257-4694

**Abstract:** This paper presents the results of an experimental investigation of fatigue response of stainless steel SS 304 L(N) and SS 316 L(N) using cyclic ball indentation test method. A Tungsten Carbide (WC) spherical ball of 1.57 mm diameter is used for applying compression-compression fatigue cycling on the test specimen having a nominal thickness of 5 mm; the displacement response is monitored as a function of every cycle of loading. The study focused on cases where the stainless steel specimens were welded by two different welding processes – Activated flux TIG welding and conventional multi-pass TIG welding. Fatigue response was monitored at locations of weld zone, heat affected zone (HAZ) and base metal to identify the effect of microstructure variation on fatigue response. It is observed that there is a steady increase in depth of penetration of the spherical indenter due to fatigue cycling; however, after a number of cycles, there is a sudden increase in depth of penetration which indicates the failure of the material beneath the indenter. The specimens after cyclic ball indentation were examined using a scanning electron microscope and one could observe the presence of secondary cracking in the penetrated region of the specimen.

**Keywords:** Cyclic ABI testing; fatigue; failure life; weld and HAZ region; SEM observations.

---

## 1. Introduction

Life prediction of safety-critical components and structures is an important task where the accuracy of predictions, reliability and confidence level are critical parameters. One of the inputs that form the basis for life extension is the data on the present condition of the material. As the volume of material available for testing from working components is limited, recourse is taken to evaluate with reasonable level of confidence the mechanical behaviour of materials using small specimen test methods. The following mechanical properties are widely estimated using small specimen test methods: tensile properties [1-4], impact [5-6], fracture toughness properties [7-8] and in a few cases fatigue properties are evaluated through sub-size hourglass specimens [9]. Fatigue crack growth experiments have been carried out using miniature specimens [10-11] to estimate the degradation in performance due to irradiation. However, experimental techniques available to evaluate the fatigue properties through in-situ test methods are limited.

Welding is one of the most common engineering material joining methods over the past several decades. Despite many advances in welding technology, welded components pose difficulties when subjected to fatigue loading. This is due to the presence of different microstructures at the weld zones compounded with the presence of residual stresses in the weld region – typically the heat affected zone (HAZ). Estimation of fatigue properties at the weld region has been a topic of research over several decades. Specimens cut across the various sections are used to estimate the plain fatigue properties of welds. These are typically butt-welded joints. The purpose of this work is to assess the fatigue behavior of weld joints for a typical structural stainless steel material through a novel cyclic ball indentation test method.

The cyclic ball indentation technique can be considered as an extension of the automated ball indentation (ABI) test technique proposed by Haggag et al [12-13] to evaluate the static properties of materials. ABI test method employs a series of programmed load-unload segments to derive the stress-strain properties, but the indentation depth keeps varying as a function time. Hence, it cannot be considered as cyclic indentation testing. Under Cyclic ABI, the cyclic indentation load is held constant. In such a case, the depth of penetration would vary with the number of cycles of loading, and this forms the basis for prediction of failure life.

Dynamic indentation studies on foam material using flat cylindrical indenters has shown that if a material is cyclically loaded using an indenter, the force-displacement response changes as a function of the number of cycles of loading [14]. A drop in displacement has been considered as the material failure parameter during cyclic indentation. A similar approach is used in cyclic ball indentation studies carried out through the experimentation route. Details such as total depth of penetration as a function of applied cycles and loading/unloading compliance derived from the force vs. displacement response, offer the scope for the assessment of fatigue behavior of a material.

## 2. Materials and Methods

Structural stainless steel SS 304 L(N) and SS 316 L(N) in base metal form, as well as in welded form are considered for this study. Cyclic ABI (fatigue) tests were carried out on a 100 kN MTS closed-loop servo-hydraulic test system (Fig. 1a) that has a computer interface for test automation and data acquisition. The working range of the force and displacement transducer was scaled down to 1/10<sup>th</sup> of its full scale range and the system tuned for reduced working ranges. A spherical tungsten carbide (WC) indenter of nominal diameter, 1.57 mm (1/16"), was inserted into a specially formed cup, and the cup was attached to a plunger. The plunger arrangement ensures that there is no-back lash at the WC indenter interface during cyclic loading of the specimen. The other end of the plunger is mounted into the standard grips of test system. The base platen that holds the specimen was mounted on the bottom grip of the test system. To measure the local displacements close to the indenter, a set of knife edges were mounted on the test fixture and a clip-on-displacement gage, having a full scale range of +/- 2.5 mm was used to measure the local displacements (Fig. 1b). The range of displacement transducer was electronically scaled down in the test controller for measurement purposes.

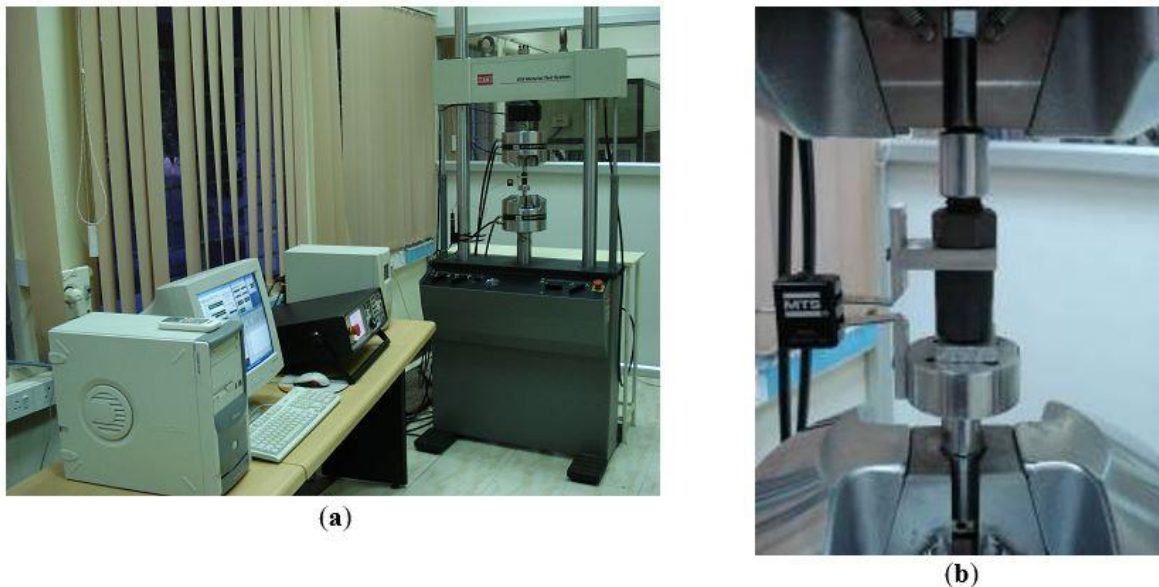


**Figure 1.** (a) Photograph of cyclic ball indentation test set-up; (b) close-up view of the spherical indenter along with clip-on-displacement gage that was used to measure local indenter depth of penetration.

The fatigue properties are estimated under compression-compression cyclic loading using sinusoidal wave form under force control mode. Test sequence for cyclic indentation was programmed to conduct tests in force control mode at a stress ratio (ratio of minimum to maximum load applied) of  $R=0.1$ . The test was conducted under constant amplitude loading investigating the cyclic load-displacement response for the base metal, Activated TIG welded region and Multi-Pass TIG welded regions of the stainless steel materials. As the plastic strain beneath the indenter is a function of the depth of penetration, different load amplitudes were chosen to obtain the plastic strain versus failure life data.

## 3. Results and Discussion

Figure 2a presents the typical load-indenter displacement response for SS 316 L(N) base metal (BM) subjected to 1000 N of peak compressive force and 100 N of minimum compression force. Also shown in the same graph is

the data for a cyclic indentation test conducted with 1250 N and 125 N as maximum and minimum force. Figure 2b presents the first cycle load-displacement data for SS 304 L(N) in base metal (BM) and Multi-Pass TiG (MP-TiG) welded conditions. It can be noted that the depth of penetration increases with an increase in peak load applied for SS 316 L(N) material. By comparing the graphs 2(a) and 2(b), one can say that the depth of penetration in SS 316 L(N) base material for the same 1000 N compressive load is lesser than that of SS 304 L(N) base material. The indentation depth is less for MP-TiG weld region of SS 304 L(N), which has a finer grain microstructure.

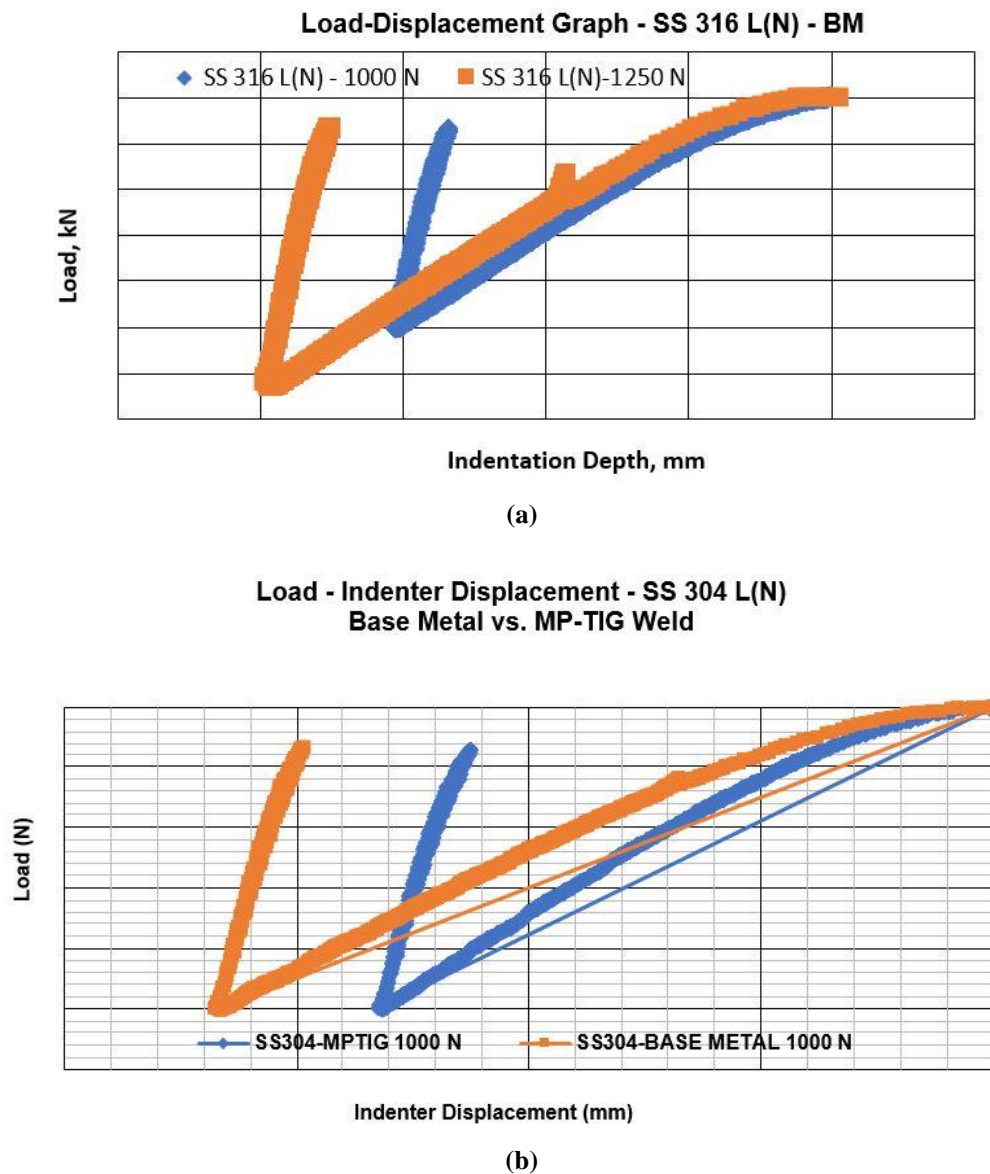


**Figure 2.** (a) Load-indentation depth for SS 316 L(N) material in base metal condition at two different loads; (b) comparison of load-indentation depth response for SS 304 L(N) material in base metal and Multi-pass TiG welded condition.

As indicated earlier, the indentation depth was monitored continuously during the test and the load-indenter depth data was logged. From this data, the unloading slope over a window covering 90-50% of peak compressive load was used for extracting the plastic depth of penetration data. Figure 3 presents the slope vs. number of cycles data for a SS304 L(N) MP-TiG weld region. It can be seen that at cycles close to N=2400, there is a change in the slope response from the previous cycles, with a sudden increase that is followed by a decrease in slope of the load-displacement data. This is characteristic of cyclic ABI testing and represents the failure of the material beneath the indenter. To understand this aspect, the specimens were electro-polished prior to the start of the experiment and after this event the specimen was examined under an optical and a scanning electron microscope to obtain details

of material beneath the indenter. Presence of extensive slip around the periphery of the spherical indenter and secondary cracking in the depth direction was observed from the SEM observations. Figure 4 presents a typical SEM image of the specimen after it was tested under cyclic ball indentation testing.

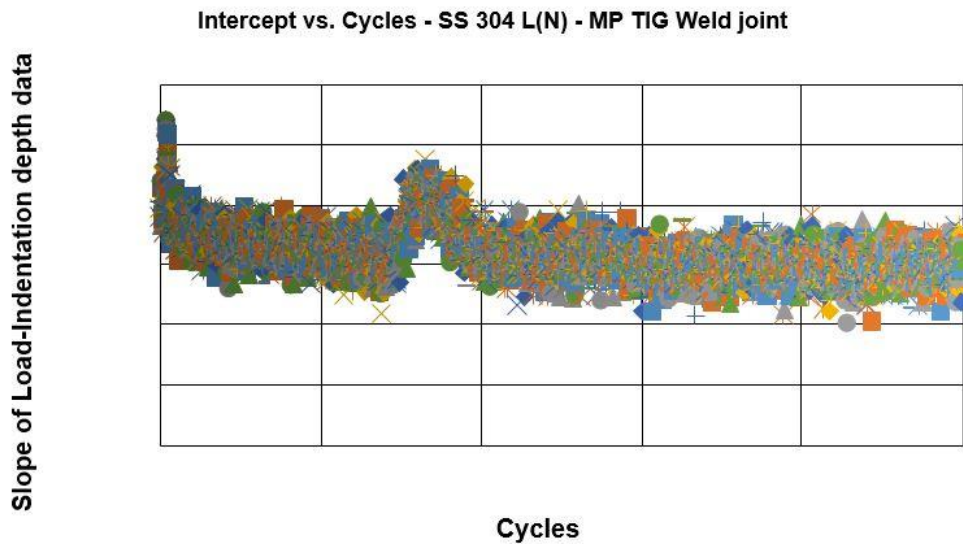


**Figure 3.** Slope of load-indentation depth data vs. cycles for SS 304 L(N) MP-TIG weld joint tested under cyclic ball indentation testing at 1500 N.

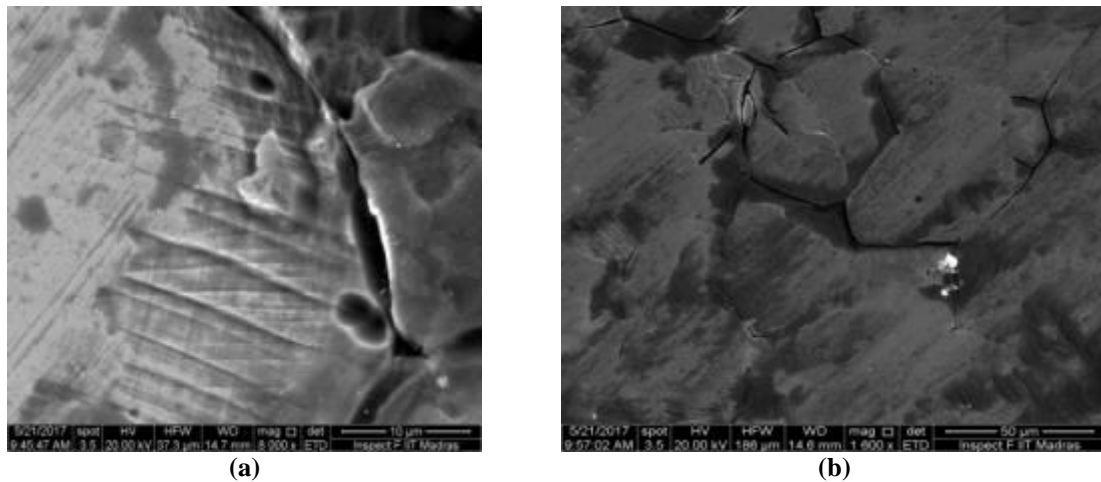


**Figure 4.** (a) Typical SEM Image near the periphery of indenter and specimen flat surface for SS 304 L(N) Base metal tested under cyclic ball indentation testing at 1250 N; (b) Typical SEM image near the mid-thickness region of indentation. Secondary cracks along the depth direction can be seen.

The cycles corresponding to the change in response of slope during cyclic indentation is collected for a number of experiments conducted at different load levels and for different microstructures. For a better consistency in tracking such data, the number of the cycles corresponding to such a shakedown has been tracked using a 2% offset from the mean intercept data and the same has been correlated with plastic strain. Figure 5 presents the graph of average true strain (obtained using Haggag’s equation [12-13] for true strain from plastic penetration depth) versus the failure cycles for the variety of cyclic ABI experiments conducted. It can be seen that there is a good strain life linear plot between the (peak) plastic strain and failure cycles as estimated through cyclic ball indentation.

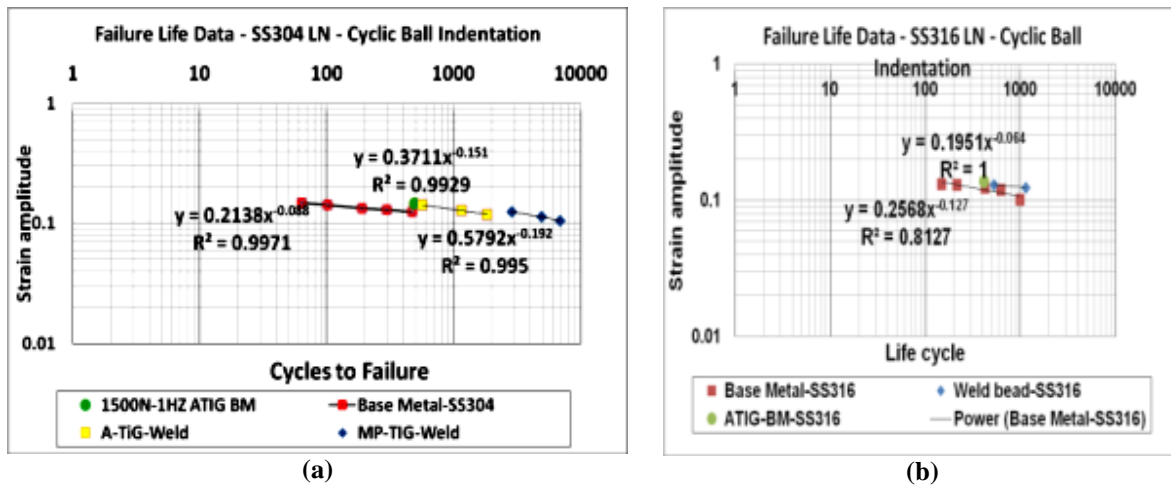


**Figure 5.** (a) Plastic strain vs. failure life data for SS 304 L(N) material in base metal, A-TIG and MP-TIG conditions; (b) Plastic strain vs. failure life data for SS 316 L(N) material in base metal, A-TIG weld conditions.

Figure 5a presents the failure life data plot as a function of strain amplitude for SS 304 L(N) material under various conditions: base metal, Activated flux-TIG (A-TIG) weld and MP-TIG weld. It is noted from the figure that the strain ductility coefficient for the MP-TIG weld region is the highest (0.579) compared to the A-TIG weld (0.371) and the least strain ductility coefficient was found for the base metal (0.2138). The strain ductility exponent for the MP-TIG weld is also the highest, thus indicating that the material is sensitive to low cycle fatigue. Figure 5b presents failure life information obtained from SS 316 L(N) material for the base metal and weld bead. The fatigue ductility coefficient of base metal is superior compared to the weld bead (based on the limited data analysis). Further experimentation is in progress to characterize the fatigue data for various strain levels.

Many of the experimental data reported here are from tests conducted at a select set of test frequencies, such as 0.1 Hz, 0.5 Hz and 1 Hz. The test results suggested that the failure life is not influenced by the test frequency. The reason for conducting experiments at different test frequencies was to ascertain if strain rate had an effect on failure life. The reason that test frequency did not show an influence could be the low rate of test frequency and possibility of heat dissipation from the specimen deformation zone to the surroundings, which annulled the strain rate effect on failure life.

It is further noted that though the failure life data is plotted in a conventional manner, the local stress ratio is not the same as the global loading stress ratio ( $R=0.1$ ) as the local deformations are very different from the global deformations. Thus, a mean stress and mean strain correction may be required to correlate this data with those obtained from fully reversed low-cycle fatigue experiments. Work is in progress to obtain such a correlation through finite element simulations of cyclic ball indentation as well as through empirical relationships. Furthermore, it is proposed to explore the cyclic ball indentation tests under displacement control, as the depth of penetration varies with the number of cycles in the present load control mode; this affects the pin-pointing of strain for failure life determination, though the drop in displacement serves as a useful indicator for failure. In case of displacement controlled fatigue, the drop in load would hopefully serve as an indicator of failure.

#### 4. Conclusions

This paper presented the results of an experimental study of cyclic ball indentation on base metal, weld region of two structural stainless steel materials: SS 304 L(N) and SS 316 L(N). From the experiments conducted at various load levels, it has been established that a typical plastic strain versus failure life data can be constructed; further, the distinction in failure life response between base metal and weld region can be clearly seen. The presence of secondary cracking as observed through SEM studies could correlate with failure tell-tale evidences from load-depth of penetration.

**Acknowledgments:** The authors thank the IITM-IGCAR Projects Cell for the support.

## References

1. Manahan, M.P.; Williams, J.; Mariakanitz, R.P., *ASTM STP1204*, ASTM International, West Conshohocken, PA, 1993, pp. 62–76.
2. Nunomura, S.; Nishijima, T.; Higo, Y.; Hishinuma, A., *ASTM STP 1204*, 1993, pp 256–266.
3. Jitsukawa, S.; Kizaki, M.; Umino, A.; Shiba, K.; Hishinuma, A., *ASTM STP 1204*, ASTM International, West Conshohocken, PA, 1993, pp. 289–307.
4. Garner, F.A.; Hamilton, M.L.; Helnisch, H.L.; Kumar, A.S., *ASTM STP 1204*, ASTM International, West Conshohocken, PA, 1993, pp. 336–355.
5. Kryukov, A.M.; Sokolov, M.A.; *ASTM STP 1204*, 1993, pp. 417–423.
6. Rosinski, S.T.; Kumar, A.S.; Cannon, S.; Hamilton, M.L., *ASTM STP 1204*, International, West Conshohocken, PA, 1993, pp. 405–416.
7. Alexander, D. J., *ASTM STP 1204*, ASTM International, West Conshohocken, PA, 1993, pp. 130–142.
8. Tomimatsu, M.; Kuwaguchi, S.; Iida, M., *ASTM STP 1329*, ASTM International, West Conshohocken, PA, 1998, pp. 470–483.
9. Hirose, T.; Tanigawa, H.; Ando, M.; Suzuki, T.; Kohyama, A.; Katoh, Y.; Narui, M., *ASTM STP 1418*, ASTM International, West Conshohocken, PA, 2002, pp. 181–194.
10. Murase, Y.; Nagakawa, J.; Yammamoto, N., *ASTM STP 1418*, ASTM International, West Conshohocken, PA, 2002, pp. 211–220.
11. Li, M.; Stubbins, J.F., *ASTM STP 1418*, ASTM International, West Conshohocken, PA, 2002, pp. 321–335.
12. Haggag, F.M.; Server, W.L.; Lucas, G.E.; Odette, G.R.; Sheckherd, J.W., *J. Test. Eval.*, Vol. 1, No. 1, 1990, pp. 62–69.
13. Haggag, F.M.; Wang, J.A.; Sokolov, M.A.; Murty, K. L., *Non-Traditional Methods of Sensing Stress, Strain and Damage in Materials and Structures*, *ASTM STP 1318*, G. Lucas and D. Stubbs, Eds. ASTM International, West Conshohocken, PA, 1997, pp. 85–98.
14. Olurin, O.B.; Fleck, N.A.; Ashby, M. F., *Scr. Metall.*, Vol. 43, 2000, pp. 983–989.